Original Paper

Cellular Physiology and Biochemistry

Cell Physiol Biochem 2003;13:271-284

Accepted: May 02, 2003

Estimation of Action Potential Changes from Field Potential Recordings in Multicellular Mouse Cardiac Myocyte Cultures

Marcel D. Halbach[1], Ulrich Egert[2], Jürgen Hescheler[1] and Kathrin Banach[1]

[1]Institut für Neurophysiologie, Universität zu Köln, [2]Neurobiologie und Biophysik, Institut für Biologie III, Albert-Ludwigs Universität Freiburg

Key Words

Microelectrode array • Action potential upstroke • Action potential duration • Cardiac field potentials • Embryonic mouse cardiomyocytes • Intracellular recording

Abstract

Background: Extracellular recordings of electrical activity with substrate-integrated microelectrode arrays (MEAs) enable non-invasive long-term monitoring of contracting multicellular cardiac preparations. However, to characterize not only the spread of excitation and the conduction velocity from field potential (FP) recordings, a more rigorous analysis of FPs is necessary. Therefore in this study we aim to characterize intrinsic action potential (AP) parameters by simultaneous recording of APs and FPs. Methods: A MEA consisting of 60 substrate-integrated electrodes is used to record the FP-waveform from multicellular preparations of isolated embryonic mouse cardiomyocytes. Simultaneous current clamp recordings in the vicinity of individual microelectrodes and pharmacological interventions allowed us to correlate FP and AP components and their time course. Results: The experiments revealed a linear relationship between AP rise time and FP rise time as well as a linear relationship between AP duration and FP duration. Furthermore a direct contribution of the voltage dependent Na^+- and Ca^{2+}-current to the FP could be identified. Conclusion: The characterization of the FP allows us for the first time to estimate AP changes and the contribution of individual current components to the AP by the help of non-invasive recording within a multicellular cardiac preparation during long-term culture.

Introduction

Extracellular mapping of cardiac excitation patterns is widely used in clinical and experimental electrophysiology to describe the sequential excitation of cardiac tissue [1, 2]. Recordings at different sites of the endocardial or epicardial surface with single electrodes [3] or with a multielectrode array [4-6] reveal the origin and spread of excitation in cardiac preparations. With these methods, the pacemaker area can be detected and characterized, not only under physiological conditions in

KARGER

Fax +41 61 306 12 34
E-Mail karger@karger.ch
www.karger.com

1015-8987/03/0135-0271$17.50/0

Accessible online at:
www.karger.com/journals/net

Kathrin Banach, Ph.D.
Department of Physiology, Loyola University Chicago
2160 South First Avenue, Maywood, IL 60153 (USA)
Tel. +1 708-216-9113, Fax +1 708-216-6308
E-Mail kbanac1@lumc.edu

the sinus nodal region, but also under pathophysiological conditions, during after-depolarizations and the resulting triggered arrhythmias [3, 7].

Besides the descriptions of the origin of excitation and the direction of excitation spread, further properties of the extracellularly recorded field potential (FP) have been largely neglected. Up to now, information on the electrophysiological properties like AP duration, upstroke velocity and contribution of different ionic currents to the AP, had to be derived from intracellular recordings. However, these techniques introduce a mechanical distortion and, like high-resolution optical mapping techniques, do not allow long-term measurements [8]. In contrast to the current interpretation of FPs recorded from cardiac cells, models have been developed for neuronal FPs that relate them to the first derivative of the membrane potential, and thus to transmembrane currents [9]. This mathematical model was also applied to substrate integrated microelectrode recordings of isolated neurons [10] and proposed for small aggregates of isolated chicken cardiac myocytes by Omura [11], although in the latter example no quantitative analysis was performed. Simultaneous recordings of FPs and action potentials (APs) in pyramidal cells and interneurons revealed that the width of the AP as well as the AP upstroke can be characterized by FP recordings based on this theoretical approach [12]. A similar analytical approach for cardiac FPs could advance the analysis of excitation spread and arrhythmic activity in multicellular preparations like the developmental differentiation of mouse embryonic stem cells [13, 14]. In the present study we investigated if changes of the AP duration and the AP upstroke within a single preparation can be obtained from FP recordings alone. The use of microelectrode arrays (MEA, Multi Channel Systems, Reutlingen, Germany) with 60 substrate-integrated electrodes, in parallel with simultaneous recordings of intracellular APs, enabled us to identify intrinsic AP parameters from FPs recorded extracellularly from multicellular preparations of isolated embryonic mouse cardiomyocytes. Additionally, based on ion replacement in the extracellular solution and ion channel blockers, we could relate specific FP waveform components to the transmembrane currents inducing them. These experimental data provide a basis for the future analysis of changes in the AP waveform and their effect on pacemaker activity and excitation spread in multicellular cardiac preparations.

Materials and Methods

Isolation of mouse embryonic heart cells

Embryonic mice (age 12.5-15.5 days post coitum) were obtained from adult black-6 mice. The mice were handled in accordance with our institutional guidelines for animal use in research. Heart cells were isolated as described previously [15, 16] and cultured in DMEM supplemented with 20% FCS, L-glutamine (2 mmol/L), and non-essential amino acids (all chemicals were obtained from Sigma-Aldrich). A drop of the cell suspension (~10^7 cells/ml) was placed on top of the electrode field of the MEA. After attachment of the cells, culture medium was added to a final volume of 800 µl. After 1 to 3 days in culture, the cells formed a confluent multicellular monolayer that usually exceeded the area of the electrode array. In some cases, areas of increased cell density could be observed where a few layers of cells were growing on top of each other. All multicellular preparations exhibited spontaneous beating activity. The cells attached firmly to the MEA and also during contractions no significant dislocations of the cells could be observed.

Current clamp recordings

APs were recorded from cells within the multicellular preparation that were located close to individual electrodes of the MEA at 21°C in the whole-cell current-clamp configuration [17] (EPC-9, PULSE software package, HEKA Electronics, Lambrecht/Pfalz, Germany) and digitized at 666 Hz. In some experiments (0-Na^+; 0-Ca^{2+}; Tetrodotoxin (TTX)), a constant beating frequency and origin of excitation spread was ensured by external stimulation. The stimulation electrode consisted of a glass micropipette filled with extracellular solution (in mmol/L: NaCl 140, KCl 5.4, $CaCl_2$ 2, $MgCl_2$ 1, HEPES 10, Glucose 10, pH = 7.4), positioned in sufficient distance to the electrode array to avoid stimulation artifacts. The preparation was stimulated with biphasic-bipolar pulses (1 ms duration each) and twice the threshold intensity with a frequency of 1.6 Hz (Grass SD9).

Patch pipettes were filled with (in mmol/L): K-glutamate 100, KCl 40, $MgCl_2$ 1, Na_2 ATP 4, EDTA 0.5, HEPES 5, pH = 7.4. In the Na^+-free solution, extracellular NaCl was substituted with the equimolar amount of LiCl. In Ca^{2+}-free solutions no calcium was added to the extracellular solution and the concentration of $MgCl_2$ was increased to 2 mmol/L.

MEA recording

For extracellular recordings of the FP from multicellular preparations of cardiomyocytes substrate-integrated planar MEAs were used [13, 14, 18-21], consisting of 60 Titanium Nitride coated gold electrodes (Ø = 30 µm; inter-electrode distance 200 µm). An Ag/AgCl electrode was inserted into the dish as reference electrode. The MEA was connected to the amplifier system (Multi Channel System, Reutlingen, Germany), which included a heating device. The characterization of the preparations spontaneous beating activity was performed at 37°C; simultaneous recordings of APs and FPs were performed at room temperature where the decreased beating frequency facilitated gigaseal formation. Data were recorded

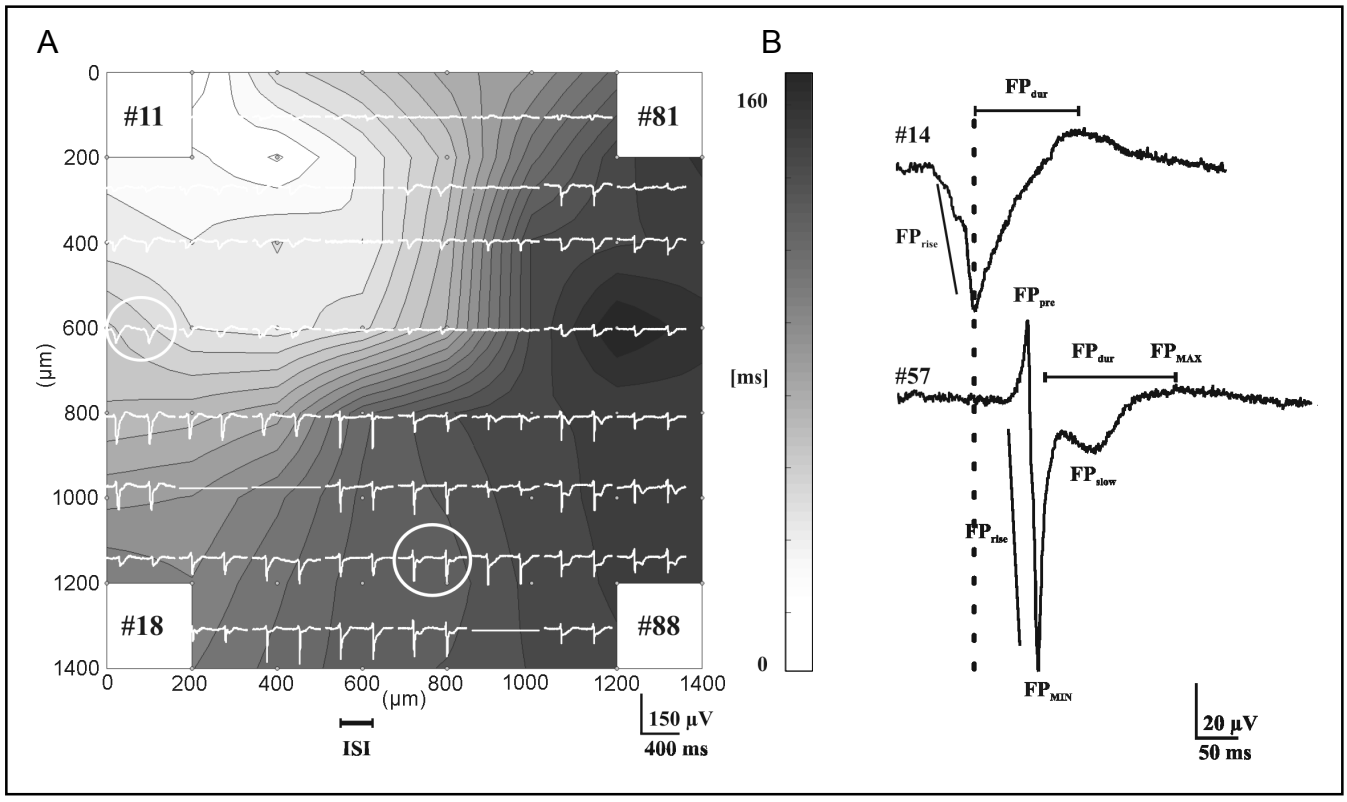

Fig. 1. Original voltage traces recorded from 60 electrodes of the MEA (A) are superimposed over a contour plot of the preparation indicating the delay of excitation spread within the preparation. The interpolation of the contour plot is based on electrodes with sufficient signal-to-noise ratio (small circles). The voltage signals are arranged according to the MEA layout, numbers in the corner positions indicate the naming scheme of the electrodes. The spontaneously active culture contracted simultaneously across the recording area. Encircled FPs are magnified in (B), illustrating representative FP waveforms. FP_{dur}, FP_{pre}, FP_{MIN}, FP_{slow} and FP_{MAX} indicate characteristic components that can be distinguished in the FP. The vertical dotted line illustrates the time delay between the appearance of FP_{MIN} on electrodes #14 and #57.

simultaneously from up to 60 channels (sampling frequency 2-4 kHz; bandwidth 1-5000 Hz, Fig. 1A). The data were analyzed off-line with a customized toolbox programmed with MATLAB (The Mathworks, Natick, MA, USA) to detect and characterize FPs [19]. The program allowed the computerized analysis of the beating frequency and additional characteristics of the FP waveform, whereas further parameters like FP_{dur}, FP_{MAX}, and FP_{slow} were introduced for the characterization of cardiomyocytes preparations, differentiated from mouse embryonic stem cells [13]. The quantitative analysis of these parameters is presented in this paper. In detail, the parameters analyzed include the size and timing of the first negative peak of the FP (FP_{MIN}) and of the last positive peak of the FP toward the end of each contraction cycle (FP_{MAX}). The duration of the FP (FP_{dur}) was defined as the time between FP_{MIN} and FP_{MAX}. The time span required for the decline of the voltage from baseline to FP_{MIN} (between 10% and 90%) was defined as the FP rise time (FP_{rise}); although a decline to a negative voltage peak is described we chose the term FP_{rise} because of its correlation to the AP rise time. Further details on the parameters used to characterize the FP are described in the results section (Fig. 1B).

In some experiments, FP_{MAX} is not always obvious to the eye. We therefore averaged FP_{dur} over a continuous recording that included ~20 successive APs. The detection usually becomes increasingly difficult as the size of FP_{MAX} decreases. Concurrently, determining the time of this peak becomes influenced by system noise. Since we wanted to determine how well FP_{dur}, which critically depends on FP_{MAX} could capture AP properties, we did not exclude FPs from the analysis based on a subjective judgment of the existence or lack of a peak, nor on heuristic threshold. We therefore included all FPs in the analysis that were detected by crossing the minimum threshold set for the detection of FP_{MIN}.

Results

FP waveform

We recorded FPs from multicellular preparations of isolated cardiac myocytes simultaneously at up to 60 different locations. In a first step, we identified

representative parameters in the FP waveform that could be detected reproducibly in FPs recorded on different MEA electrodes within a single preparation as well as in different MEA preparations. In the preparation shown in Fig. 1A spontaneous electrical activity was recorded from a synchronously contracting multicellular preparation at day 4 in culture. Different characteristic waveforms could be detected on different electrodes. Two representative examples are magnified in Fig. 1B. The onset of the FP could either be continuous and slow, as seen for example in the FP of electrode number 14 (#14), or a more rapid decline to a negative minimum (FP_{MIN}) could be observed, which was sometimes preceded by a positive pre-spike (FP_{pre}) as seen on #57 (bottom panel). After reaching FP_{MIN}, the potential either slowly but continuously rose to the baseline and proceeded to a more or less pronounced positive peak (FP_{MAX}; see #14), or rose rapidly but then reverted into a second, slowly declining, negative peak (FP_{slow}; #57) before the final FP_{MAX}. Not in all cases FP_{slow} is separated from FP_{MIN} by the incision seen in this example, but as in this example a plateau like phase can be distinguished.

The FP shape depends not only on local transmembrane currents, but also on passive circuit currents, induced by simultaneously excited tissue connected to the recording site predominantly through ohmic conductance [22]. This tissue may even be distant to the recording site [9, 22-24]. One example of these currents is FP_{pre}, an outward current occurring simultaneously with the depolarization of neighboring membrane sections or electrically coupled surrounding cells. Depending on the intercellular resistances these outward currents may be distributed unevenly across different cells connected by gap junctions. As proposed for cardiac as well as neuronal cells, these currents are one of the components adding to regional differences of the FP waveforms detected within a multicellular preparation [12, 24]. To distinguish the active current components, related to ionic currents, from the passive, largely capacitive, current components, we performed current clamp recordings on single cells within the multicellular preparation. The recording sites were selected in the close vicinity of a MEA electrode (up to 30 µm) and FPs from the same electrode were recorded simultaneously to the AP recordings.

In all paired recordings, (N=55) the onset of the AP correlated well with the deviation of the FP from the baseline to $FP_{MIN.}$ The peak of FP_{MIN} always preceded the maximal depolarization of the AP and FP_{rise} appeared to depend on the rise time of the AP (Fig. 2A, N = 50 paired recordings from 15 cultures). In the interpretation of the FP as related to the 1st derivative of the AP, this would translate such that FP_{rise} is proportional to the duration of the AP upstroke during the time period before V_{max} resulting in FP_{rise}<AP_{rise}. In Fig. 2A FP_{rise} is plotted

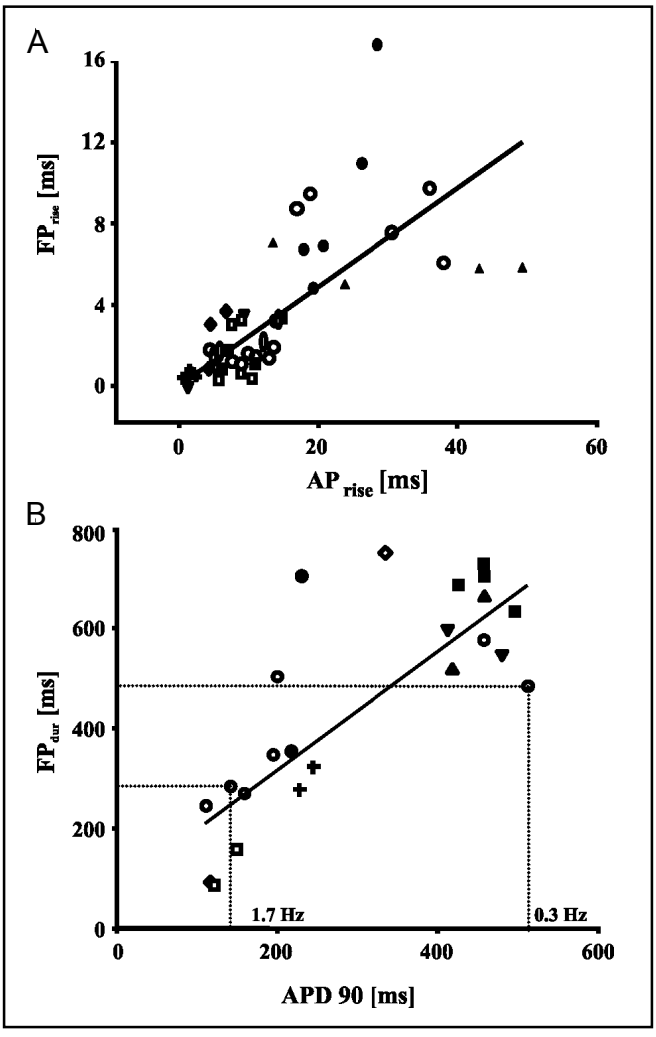

Fig. 2. (A) FP_{rise} and AP_{rise} were highly correlated in paired recordings of intracellular APs and extracellular FPs obtained at room temperature from spontaneously beating cultures (r=0.81, 50 paired recordings from 15 preparations). (B) FP_{dur} was correlated with APD90 (r=0.86, 33 paired recordings from 14 preparations). Variations in the length of the APD90 correlated with the spontaneous beating frequency of the preparation where high frequencies were associated with shorter APD90s. In both plots each individual point represents the mean value of 20 consecutive APs and FPs respectively, with matching symbols representing measurements that were obtained from different locations within the same culture. Open circles represent experiments where only one recording was obtained from a preparation.

as a function of AP_{rise}; each point in Fig. 2A represents the mean value obtained from the analysis of ~20 consecutive APs in one continuous recording. No distinction was made between different FP waveforms but all measurements were included in the plot. FP_{rise} was indeed shorter than AP_{rise}, and strongly correlated with it (r = 0.81; slope= 0.256).

Similar to AP and FP recordings in neuronal cells, a close correlation of the repolarizing phase of the APs with FP_{MAX} was characteristic for all recordings. To compare AP duration and FP duration (FP_{dur}) we defined FP_{dur} as the time between FP_{MIN} and FP_{MAX} and the AP duration as the time of 90% repolarization (APD90). Plotting FP_{dur} as a function of APD90 (Fig. 2B) demonstrates the close correlation between both parameters (r = 0.86; slope = 1.18; N = 33 paired recordings from 14 cultures). APD90s ranged from 100 to 500 ms. This variability could be due to culture dependent differences in the beating frequency which ranged from 1.7 to 0.3 Hz; where low beating frequencies correlated with extended APD90s (Fig. 2B).

Electrical coupling within the multicellular preparation of cardiac myocytes is indicated by the frequency entrainment of the cells [5, 25, 26] and propagation of excitation. To ensure further that the AP recorded in one cell of the preparation is representative for at least the cells in the surrounding of the electrode we successively recorded APs at different locations around the same MEA electrode. Two examples of such successive recordings are shown in Fig. 3Aab and 3Bab. Although the cells recorded intracellularly were located at different positions in the surrounding of the same MEA electrode (eg. 3Aa and 3Ab) the APs recorded from these cells were comparable and the FP recording from the MEA did not change during the recording. These data underline, that electrical coupling within the multicellular preparation of cardiac myocytes enables not only frequency entrainment of the entire preparation, but also the waveform entrainment at least across certain areas of the preparation. We therefore conclude that the FP parameters FP_{dur} and FP_{rise} are proportional to APD90 and AP_{rise} respectively, and can be utilized in FP recordings of multicellular preparations of cardiac myocytes to monitor changes of these properties over time in culture or during pharmacological interventions.

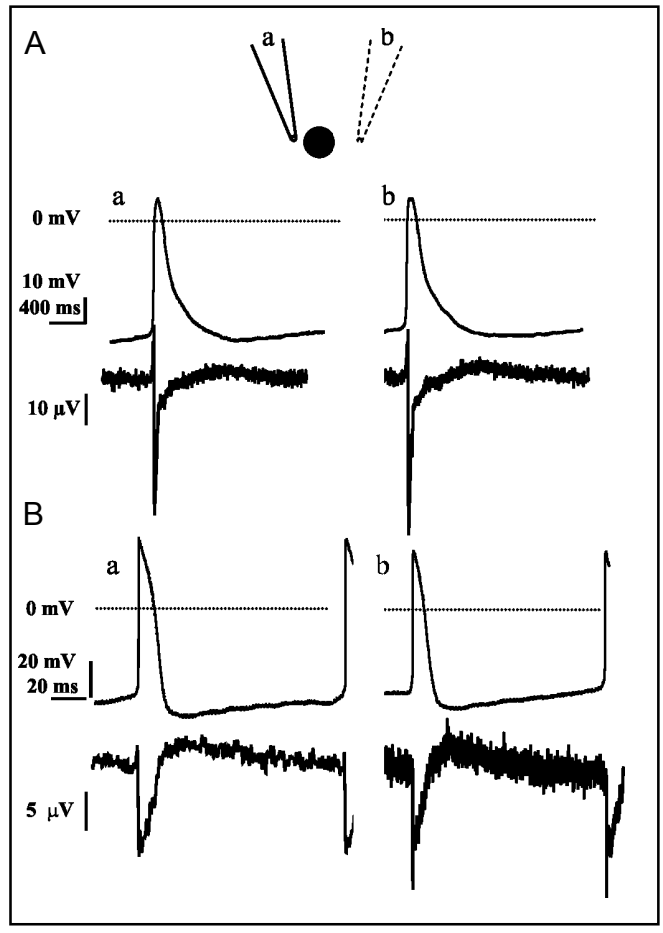

Fig. 3. Paired recordings of APs (upper trace in each panel) and FPs (lower trace in each panel) in spontaneously active cultures. Whereas FP_{MIN} correlates in time with the AP upstroke, the repolarization of the AP coincides with FP_{MAX}. APs (Aa and Ab) were recorded successively from different cells around the same MEA electrode. The FP recorded simultaneously from this same MEA electrode is shown underneath. The examples shown in (Aab) and (Bab) were obtained from different MEA electrodes and cultures. In both cases the successively recorded APs were very similar (A (a/b): APD90: 428 ms/459 ms; AP_{rise}: 24 ms/23.25 ms, B (a/b): APD90: 157.3 ms/ 124.5 ms; AP_{rise}: 3 ms; 3.5 ms) pointing to the waveform entrainment of the preparation.

Culture dependent differences in the FP

As indicated above, the shape of FPs measured on different electrodes within a single preparation varied (Fig. 1AB). To determine if FP waveforms depended on differences between cultures, we recorded the spontaneous electrical activity of different preparations on successive days in culture (39 recordings from 13 preparations). The beating frequencies as well as FP_{dur} were analyzed as a quantitative measure for the electrophysiological properties of the preparations (Fig. 4AB). Spontaneous electrical activity could be detected from the first day in culture, inter-spike interval (ISI) and

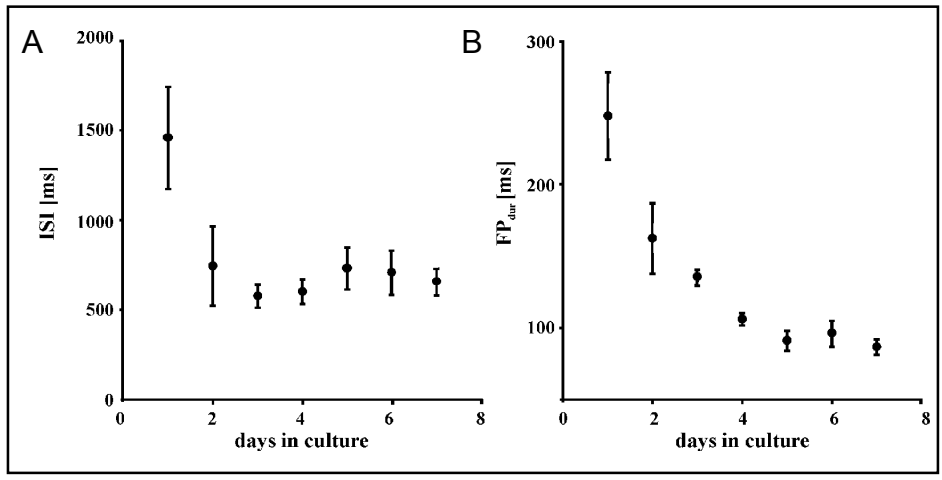

Fig. 4. ISI (A) and FP_{dur} (B) are plotted as a function of the preparations days in culture (39 measurements from 13 cultures in each plot). Each data point represents the mean ±SEM of different spontaneously beating preparations. ISI as well as FP_{dur} decrease during the first 2-3 days in culture. In both cases the decline was independent of the embryonic age of isolation.

FP_{dur} decreased during the first two to three days and remained stable afterwards. The values obtained and their time course was very reproducible across different cultures. Thus FP variability as a consequence of a dedifferentiation process has to be considered during the first days after isolation, nevertheless it seems to affect cultures on different MEAs equally indicating that variability of the individual MEAs is not an issue.

Regional distribution of FP parameters

To characterize further the properties of the different FP waveforms we analyzed their spatial distribution within the spontaneously active multicellular preparations (N=9). Starting from the location where the earliest FP or FP_{MIN} was recorded, we determined the delay of FP_{MIN} during a contraction cycle on the remaining electrodes of the MEA (Fig. 5A). FP_{dur} and FP_{rise} were analyzed for electrodes located along the path of the major wavefront of excitation spread. The results were plotted as a function of distance of each electrode from the origin of excitation on the MEA. An example is shown in Fig. 5DE. The contour plot of this preparation revealed that the excitation spread continuously over almost the entire electrode field starting out simultaneously at electrodes #17 and #28. Although the FPs recorded from the electrodes analyzed (Fig. 5B) varied in their amplitude, they exhibited an overall similar characteristic waveform. For all FPs selected FP_{MIN} is preceded by FP_{pre}, indicating a contribution of neighboring, previously excited tissue [23, 27]. After reaching FP_{MIN}, all FPs exhibit the prolonged second negative plateau like component FP_{slow}, already described in Fig. 1B. The analysis of FP_{dur} confirmed this similarity; no significant variation of FP_{dur} (Fig. 5C) could be detected along the path of excitation spread. To enable the comparison of different preparations we normalized the variation of the FP_{dur} according to the longest FP_{dur} measured in each preparation and plotted the data as a function of the distance from the first electrode. Also in this case (Fig. 5C insert) the FP_{dur} did not change significantly. The same analysis was performed for FP_{rise}; for the preparation shown (Fig 5AB) FP_{rise} varied between 1 ms and 6 ms. Despite these variations, no clearly defined spatial distribution of this parameter could be determined. Plotting the mean value of the normalized FP_{rise} of 6 different preparations revealed a similar picture (Fig. 5D insert); however, it has to be mentioned that in contrast to all other value pairings, the value recorded at position 800 was significantly different to the last three values recorded ($P<0.05$).

In 4 different preparations regional variations of FP parameters in the direction of excitation spread could be observed. An example is shown in Fig. 6. In this preparation, the cells covered only the lower half of the electrode array. Excitation started at electrode #68 and spread smoothly towards #14 (Fig. 6AE). The FPs recorded from the electrodes marked are shown in Fig. 6B. In this case, the FP recorded at the origin of excitation (#68) descended to FP_{MIN} slowly, without a preceding FP_{pre}. FP_{slow} could not be discerned. In contrast, all FPs recorded further along the path of excitation spread exhibited FP_{pre}, as well as the negative components FP_{MIN} and FP_{slow} (Fig. 6B). Quantitative analysis of the FPs revealed that FP_{dur}, as in the cases described above, did not change significantly along the path of excitation spread (Fig. 6C). In contrast, FP_{rise} changed markedly (Fig. 6D). Whereas the values measured for FP_{rise} at the more distant electrodes (#57, #47, #36, #25, #14) are comparable to those shown in Fig. 5D, FP_{rise} at the origin

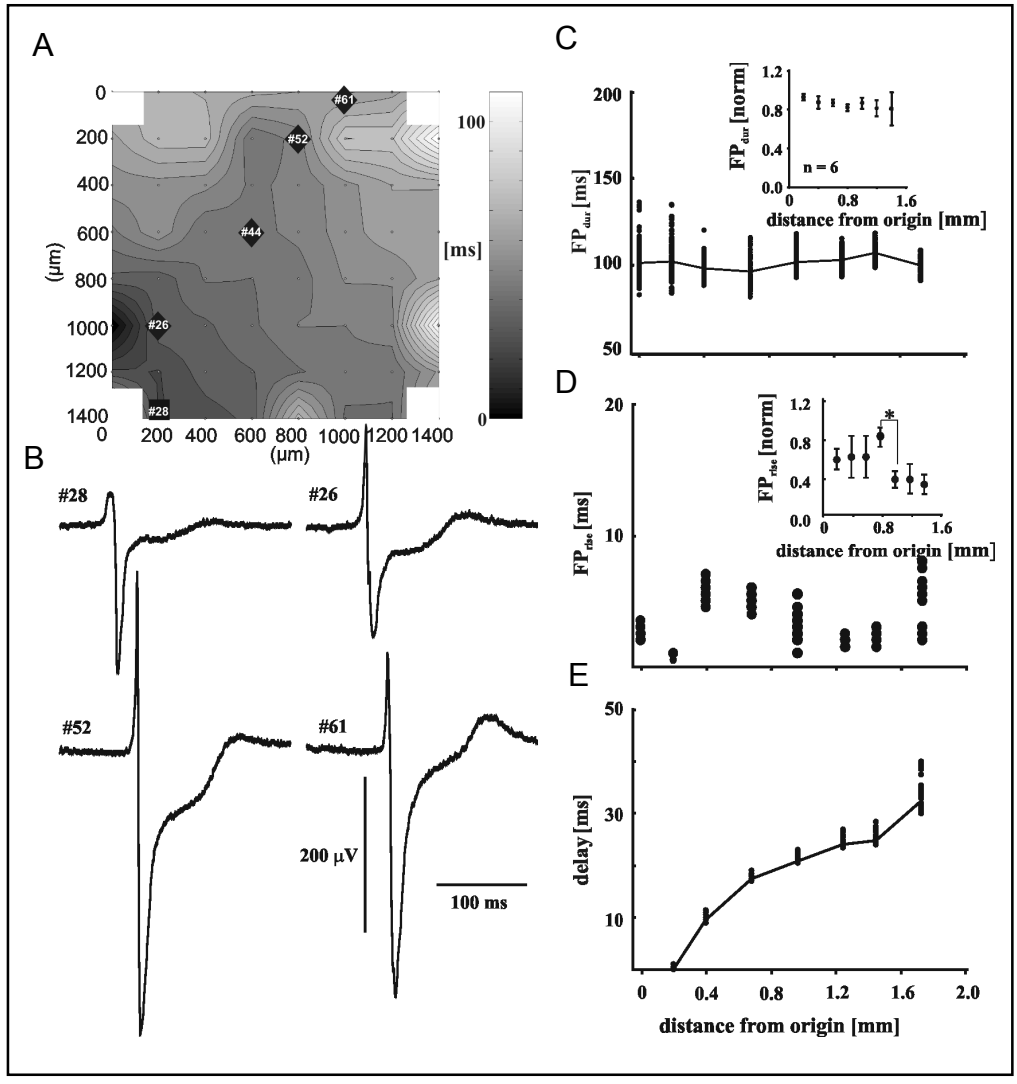

Fig. 5. Two-dimensional analysis of excitation spread and FP parameters. (A) Contour plot from a spontaneously contracting preparation that covered almost the entire electrode field. The greyscale is encoded on the right side of the plot. The black square indicates the site of the first excitation on the MEA, black diamonds represent the electrodes analyzed along the excitation wavefront. FPs recorded from the same electrodes are shown in (B). FP_{dur} (C), FP_{rise} (D) and the delay of FP_{MIN} (E) are plotted as a function of their distance to the reference electrode, i.e. the electrode exhibiting the first excitation. Every cluster of points represents consecutive FPs during a 40 s recording. The inserts in (C) and (D) show the normalized change of FP_{dur} and FP_{rise} respectively, along the path of excitation spread (mean±SEM) for 5 different cultures. In (D) the value at distance 0.8 mm varied significantly (*, $P<0.05$) form the following data points.

of excitation (#68) is markedly extended. To compare the regional differences of FP_{rise} between these 4 MEA preparations, we normalized FP_{rise} to the value recorded at the origin of excitation. On average, FP_{rise} was 5-times larger at the origin of excitation than along the propagation path (N = 4, Fig. 6D, insert). The distribution of these FP parameters along the path of excitation spread indicates that specific FP waveforms represent specific, functionally different APs, e.g. the slow depolarization of a pacemaker AP is reflected in a comparatively larger FP_{rise} of the FP.

Contribution of different ion currents to the FP

The rise time of the cardiac AP and the APD90 are determined by the sequential activation of specific ion channels [7, 28-30]. The extracellularly recorded FP depends directly on these local transmembrane currents as well as on their associated circuit currents [9, 10, 22]. To examine which parts of the FP are influenced directly by specific transmembrane currents, we performed experiments with the specific sodium channel blocker TTX and the L-type calcium channel blocker Nimodipine, as well as with ion replacement in the extracellular solution. Since passive current components influencing the FP correlate in their size and shape with the velocity of excitation spread [23, 31] and the direction of excitation spread in relation to the orientation of the muscle fiber [27], we introduced an external stimulation electrode to enforce a constant beating frequency (1.5 Hz) and a reliable origin of excitation during some experiments. We thus ensured that changes detected in the FP waveform were due to changes of the transmembrane current and not to changes in the overall direction of excitation spread.

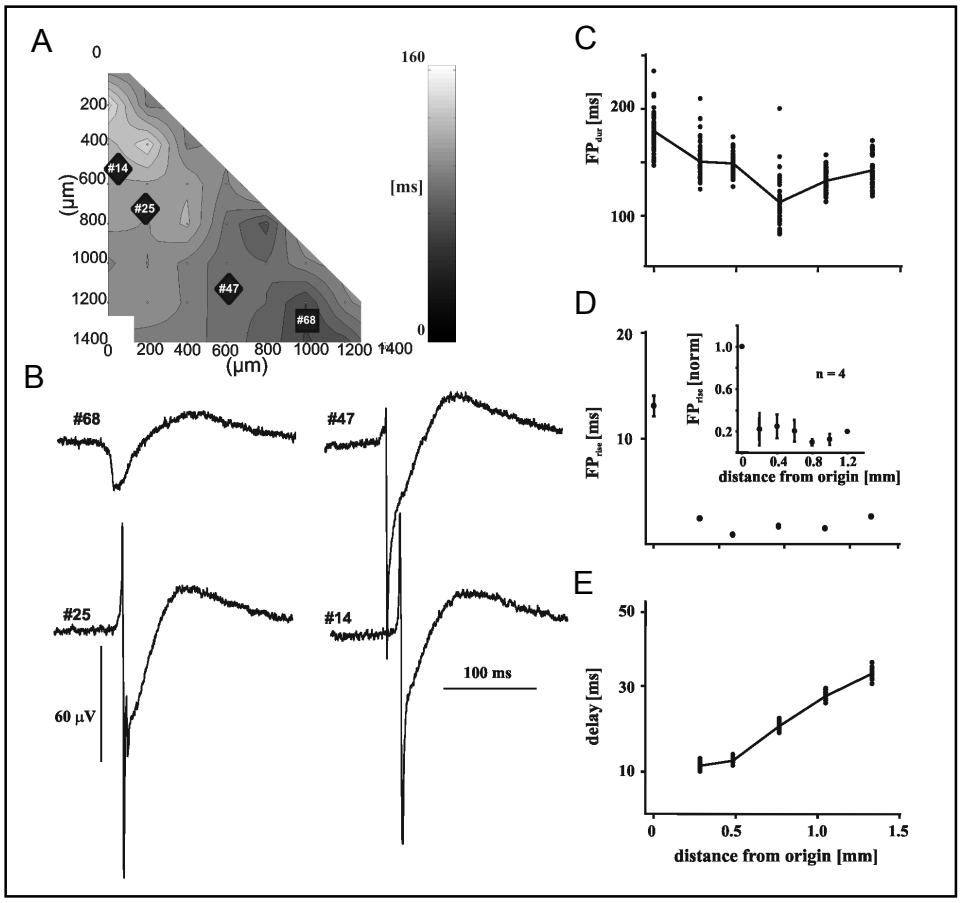

Fig. 6. Two-dimensional analysis of excitation spread and FP parameters. (A) Contour plot of the delay of excitation spread as described in Fig. 5 for a preparation covering the lower left diagonal of the MEA. The square represents the electrode determined as the origin of excitation whereas the diamonds represent the electrodes (FPs are displayed in B) analyzed along the major wavefront of excitation spread. FP_{dur} (C), FP_{rise} (D) and the delay (E) are plotted as a function of their distance to the reference electrode. In (C) and (E) each cluster of points represents individually analyzed consecutive APs recorded over a period of 30 s. In (D) the result of the analysis of the individual APs is plotted as mean±SEM. The insert in D shows the normalized change of FP_{rise} along the path of excitation spread averaged for 4 different cultures.

Sodium-dependent currents

Blocking the voltage dependent Na^+-channel in preparations of the neonatal rat heart decreased the AP's upstroke velocity, the velocity of excitation spread and increased the intracellular Ca^{2+}-load [8, 28, 32]. We tested the contribution of Na^+ to the FP by superfusion of the preparation with Na^+-free solution (substitution of Na^+ with Li^+, N=3 different preparations) or TTX (3 different preparations). Characteristic changes in the FP waveform could be observed: Na^+-withdrawal decreased FP_{MIN} (Fig. 7Ab). Na^+-free solution had the opposite effect on FP_{slow}, eventually resulting in FP_{slow} becoming more negative than FP_{MIN} (Fig. 7Ac). Concurrent to the decline of FP_{MIN}, FP_{rise} increased in this preparation from 0.65 ms to 0.9 ms, indicating a prolonged rise time of the underlying APs. The average decrease of FP_{rise} recorded from 11 electrodes in these preparations was 48.4 % ± 10.1 SEM. Similar results were obtained when the voltage dependent Na^+-current was blocked with TTX. Examples from two experiments are shown (1-50 µM; Fig. 7CD). A decrease of FP_{MIN} could be observed when FPs recorded on the same electrode during control and 1 min after application of 1 µM TTX were superimposed (Fig. 7C). For a different preparation, Fig. 7D shows the delay of FP_{MIN} along the propagation path plotted against each electrodes distance from the origin of excitation. The preparation was spontaneously active and the direction of excitation spread remained uninfluenced by the pharmacological intervention, rendering it unnecessary to introduce an external stimulation electrode in this case. TTX application resulted in a reversible ~2-fold increase of the delays between these electrodes. This result is in agreement with reports that the strength of the Na^+-current and the propagation velocity are strongly linked [8].

Na^+-currents availability can also be reduced by a depolarization of the resting membrane potential with increased extracellular $[K^+]$ [8]**.** In our preparation this led to a reduction of FP_{MIN} and a concomitant increase of the delay of excitation spread (N=4). Figure 8 illustrates the effect of an elevated extracellular $[K^+]$ on FP_{rise} (A), delay of excitation spread (B) and FP_{MIN} (C) in a spontaneously active preparation. The delay was measured for electrodes #14 and #24 relative to #44. In agreement with the experiments described above, the

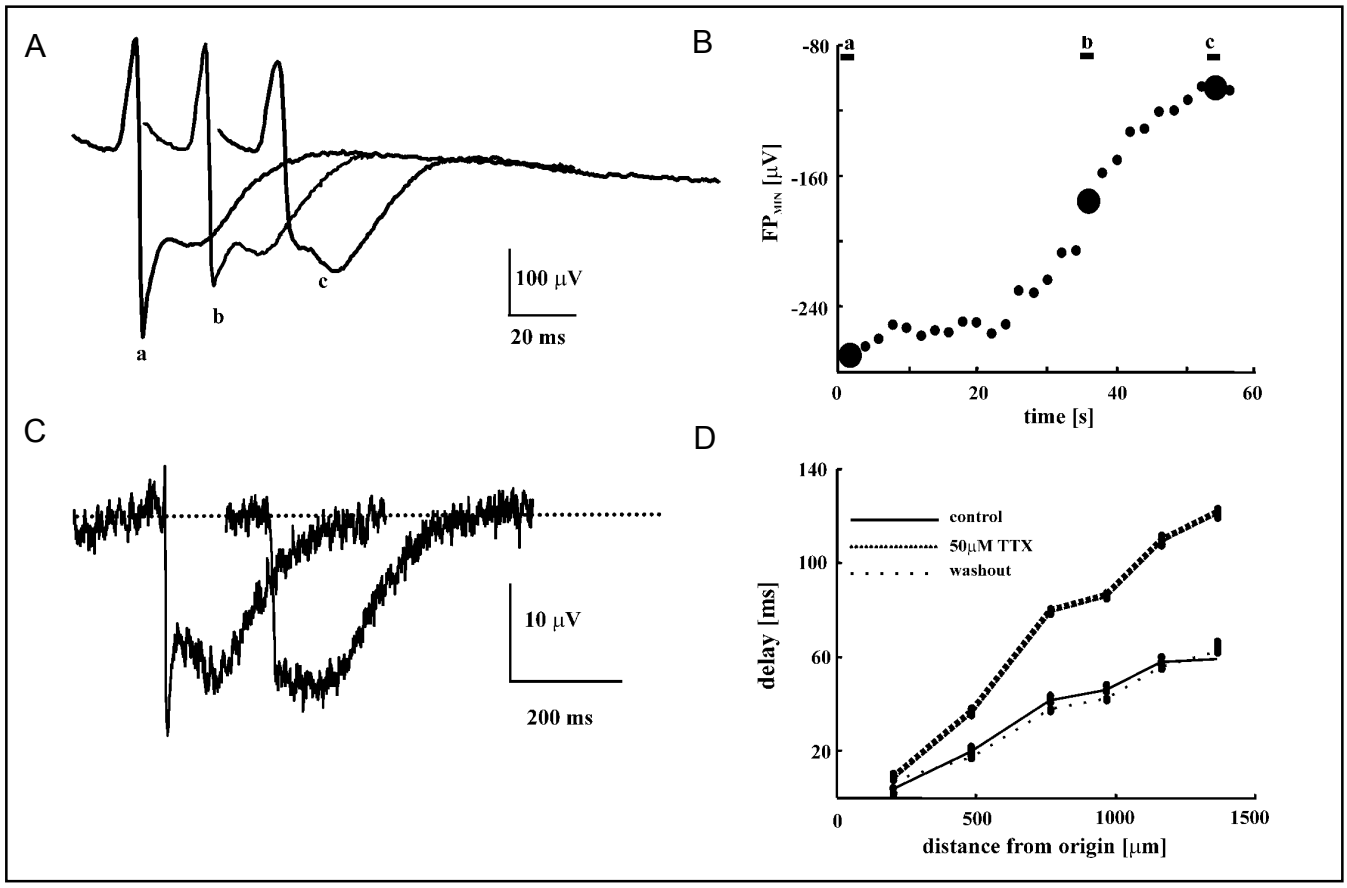

Fig. 7. (A) FPs recorded on one MEA electrode at different points in time during the superfusion of an electrically stimulated culture with 0-Na^+ solution. In (B) FP_{MIN} of the FPs shown in (A) is plotted against time. (C) A comparable change of FP_{MIN} was observed in another culture during the superfusion of 1 µM TTX. FPs were recorded before and 1 min after application of TTX from the same electrode. In (D) the delay of FP_{MIN} on electrodes along the excitation wavefront is plotted vs. the reference electrode analyzed before, 6 min after application and 12 min after the washout of 50 µM TTX. Each cluster of points represents the results of consecutive FPs recorded over a period of 30 s. Although the delay was significantly increased in the presence of TTX no change in the direction of excitation spread was observed.

reduced contribution of the Na^+-current to the FP was reflected in an increase of FP_{rise}, concomitant with a decrease of FP_{MIN}. In addition, the delay between electrodes increased, likely reflecting a decreasing conduction velocity. The results demonstrate that changes in the contribution of the Na^+-current to the AP result in changes of the parameters FP_{MIN} and FP_{rise} and the delay of excitation spread. In consequence, during an experiment relative changes in the contribution of the Na^+-current can be characterized directly from extracellular recordings of the FP.

Calcium current

The AP duration in cardiac cells is determined in part by the activation of the low voltage activated ($I_{Ca,L}$) and the high voltage activated ($I_{Ca,T}$) Ca^{2+} channel [28, 33, 30]. To characterize the contribution of $I_{Ca,L}$ to the FP we superfused the preparation with nominally Ca^{2+}-free solution (2 different preparations). FPs recorded from two different electrodes at successive points in time during the superfusion with Ca^{2+}-free solution are shown in Fig. 9AB. Both FPs exhibited a pronounced FP_{pre}, and a small peak separating FP_{MIN} from FP_{slow}. In both examples, FP_{slow} was highest in the trace recorded in control solution. Removing extracellular Ca^{2+} decreased the size of FP_{slow}, until it eventually vanished completely, while FP_{MIN} remained almost unaffected. Simultaneously, the FP_{slow} following FP_{MIN} became more positive and finally merged with FP_{MAX}. Overall, FP_{slow} decreased on average by 42.4 % ±4.8 SEM on 26 electrodes analyzed from 2 different cultures. FP_{MAX} also decreased during the removal of extracellular Ca^{2+}, which rendered its

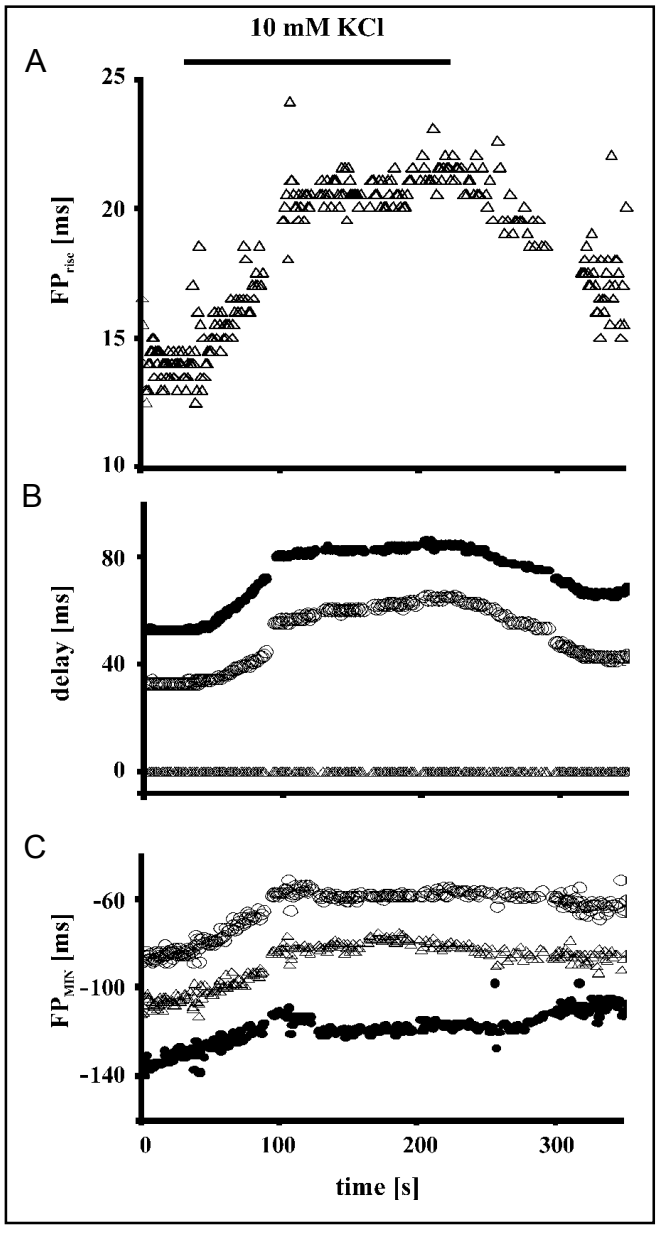

Fig. 8. (A) FP_{rise}, (B) the delay of excitation spread and (C) FP_{MIN} analyzed from a spontaneously beating preparation during superfusion with 10 mM KCl. The increase of FP_{rise} and the concomitant decrease of FP_{MIN} shown for the reference electrode (Δ) results in an increase in the delay of excitation spread between the reference electrode and two electrodes along the excitation wavefront (● and O). Each individual point in the recording represents a single analyzed FP.

detection more difficult. In most FPs examined, FP_{dur} increased during superfusion with Ca^{2+}-free solution before finally dropping to a markedly reduced value when FP_{slow} was abolished. In a second approach to this issue, we tested the effect of Nimodipine (2 nM) on the FP waveform (N=4). In all cases a reversible reduction of FP_{dur} was observed (Fig. 9C). The results substantiate the interpretation that changes of FP_{slow} directly reflect changes of the contribution of the Ca^{2+}-current to the AP.

Discussion

Although recordings of extracellular FPs have a long history in cardiac electrophysiology, the interpretation of these signals was mostly limited to the analysis of the beating frequency and the direction of excitation spread [14, 20, 34, 35]. In the present study we demonstrated that the FPs recorded from multicellular preparations of isolated mouse cardiomyocytes contain information about the AP rise time, the AP duration and individual transmembrane currents of the cells covering the electrodes. As we stated previously [13] these information do not allow us to derive an absolute measure of individual ion currents contributing to the AP but changes in the FP shape can be related to changes in the ionic currents.

Interpretation of the FP

In simultaneous recordings of intracellular APs and FPs we demonstrated that FP_{MIN} precedes the maximal depolarization of the AP and that its amplitude depends critically on the current through voltage dependent, TTX sensitive Na^+-channels (Fig. 7CD and Fig. 8). These findings support the theory that the FP parallels the 1st derivative of the intracellular AP, created by the capacitance of the membrane covering the external electrode [9-11]. According to this interpretation, FP_{MIN} corresponds in time with the time of the maximum upstroke velocity of the AP (V_{max}). Since V_{max} depends critically on I_{Na}, we replaced extracellular Na^+ by Li^+. Although this reduces, but does not block the current through the voltage dependent Na^+-channels in single cell preparations [36, 37], the data recorded in 0-Na^+ solution (Fig. 7AB) are comparable to those obtained in the presence of TTX (Fig.7CD). The effect of the Na^+-free solution might be based on the increase in membrane potential and reduced AP amplitude also reported in single cells under these conditions [37]. In agreement with our findings, a correlation of FP_{MIN} and V_{max} could be demonstrated in neuronal cell cultures [12] and Yamamoto et al. [24] described decreased FP amplitude and a lack of the first rapid deflection in the FP (here referred to as FP_{MIN}) after application of TTX to the isolated rabbit sinus

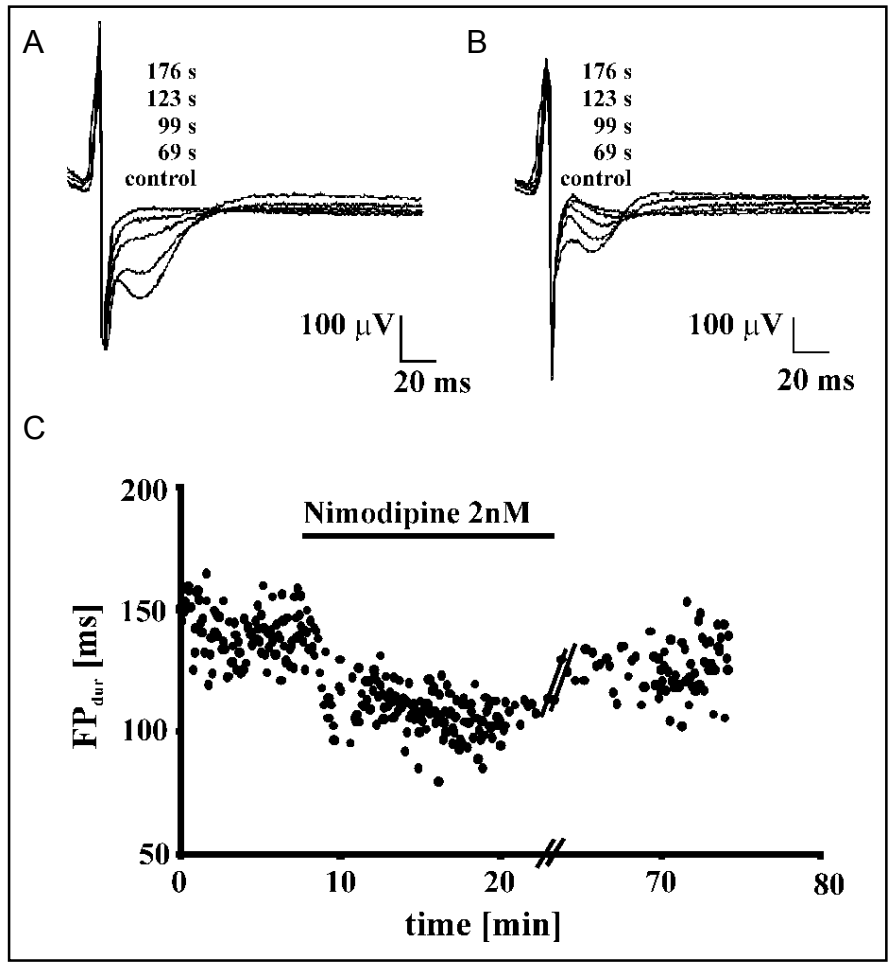

Fig. 9. (A, B) Representative FPs recorded from two electrodes during superfusion of the preparation with Ca^{2+}-free solution (time in Ca^{2+}-free solution as indicated). FP_{slow} decreased continuously during the washout of extracellular Ca^{2+}. In a different experiment, a reversible reduction of FP_{dur} was observed during superfusion with Nimodipine, a blocker of the L-type Ca^{2+}-channel (C). Each data point represents one FP; the two vertical lines indicate a 40 min interruption of the recording.

node. Their analysis was, however, hampered by changing directions of excitation spread and a low spatial resolution.

Rise time of AP and FP

In cardiac myocytes, the upstroke velocity of the AP is a characteristic feature of individual cell types, deciding their ability to generate spontaneous electrical activity and function as a pacemaker [3, 28, 30, 38]. With FP_{rise} we identified a component of the FP that correlates linearly with the rise time of the AP. FP_{rise} changed under conditions known to change the upstroke velocity of the cardiac AP such as application of TTX, depolarizing conditions and Na^+-free solution [14]. A similar correlation was obtained by Spach et al. [31] by measuring the time from the positive peak of FP_{pre} to FP_{MIN}. Our data demonstrate further that, FPs at the origin of excitation on the MEA exhibited an increased FP_{rise} in comparison to the rather uniform FPs along the path of excitation spread. This indicates that on these occasions the slower depolarization of the pacemaker region is reflected in the FP in otherwise homogeneous preparations. The lack of FP_{pre} in these FPs, which was reported to represent surrounding previously excited tissue [23], supports this hypothesis. Correspondingly, slowly declining FPs in isolated rabbit sinus node were previously interpreted to represent the origin of excitation [34, 35, 39]. In these reports, the lack of FP_{pre} and the slow decline of the FP were used as qualitative indicators of the pacemaker region.

Duration of AP and FP

In contrast to the rapid depolarization of the AP, the repolarization is based mostly on comparatively slowly activating outward currents. On the same theoretical basis as described above these currents should result in a positive deflection of the FP, which we identified as FP_{MAX}. Although we have not yet isolated the current underlying FP_{MAX}, we could demonstrate that the time interval between FP_{MIN} and FP_{MAX} correlates with the APD90 of the APs measured simultaneously at the same location. This finding, which, to our knowledge, was not previously described for cardiac cells, is in good agreement with

data from Henze et al. [12] who demonstrated a correlation of AP duration and FP duration in different types of neuronal cells. In a previous study with simultaneous intra- and extracellular recordings in the isolated rabbit sinus node, the second, slow, negative component of the FP, here referred to as FP_{slow}, was ascribed to the repolarization of the AP [24], but no correlation of FP durations with simultaneously measured AP durations was obtained. However, the change of the parameter FP_{dur} upon application of Nimodipine or application of 4-aminopyridine [13], conditions well known to either shorten or prolong the cardiac AP [28, 32, 40, 41] underline, that FP_{dur} is a valid parameter to monitor experimental changes in AP duration.

While FP_{MIN} and FP_{MAX} correlated well with the first derivative of the AP, as was also described for neuronal cells [12], FP_{slow} is not very pronounced in the derivative. Although currently this discrepancy cannot be clarified, we demonstrated that FP_{slow} gradually diminishes in 0-Ca^{2+} solutions. Since we assured a constant frequency and origin of excitation by external stimulation of the preparation, we could exclude that the change of FP_{slow} in the 0-Ca^{2+} experiments was due to a change in the overall direction of excitation spread and therefore i.e. does not reflect changes of passive currents. We propose accordingly, that FP_{slow} depends on a Ca^{2+}-inward current.

FP interpretation and the homogeneity of the preparation

In the chicken embryo, future atrial and ventricular cells can be functionally distinguished by their beat rate after isolation of the respective regions from the tubular heart at stage 5 of embryonic development [42]. In our preparation we did not attempt to separate atrial and ventricular tissue. Although the cells were isolated between day 12.5 and 15.5 of embryonic development and developmental differences in the cells electrophysiological properties were described for single cell preparations [35, 43, 44], no interdependence of the spontaneous activity and the embryonic age of isolation could be detected in the multicellular preparation. These results suggest a dedifferentiation of the isolated cells under the present culture conditions, independent of the embryonic age at which the cells were collected. The averaged data from 13 preparations demonstrate the inter-culture comparability and the stability of the preparation over time.

However, a heterogeneous assembly of the different cell types isolated must be assumed for our cultures. Whether different excitable cells exhibit their individual, cell type specific APs in a multicellular assembly depends on the intercellular resistance between them. It is well established that in two independent, spontaneously beating cells, increasing intercellular conductance results first in the frequency entrainment of the cells and, furthermore, in the entrainment of the AP waveform [25, 26]. In our preparation, measurements of the intracellular AP at different positions around a single electrode (Fig. 3) indicate that the intercellular coupling allows frequency entrainment of the entire and waveform entrainment at least in compartments of the preparation. In consequence it seems reasonable to assume that the source population of our FPs is sufficiently homogeneous for the interpretation of FPs from electrically coupled multicellular preparations put forth in this report.

Technical limitations

As addressed above, the interpretation of the FP proposed in this article relies on the assumption, that the majority of the cells contributing to the FP at a single electrode are homogeneous. However, it is necessary to distinguish between local and global homogeneity and consider the range across which an extracellular electrode integrates the electrical field, as well as the conductance between the cells. From recordings in brain slices we know that electrodes of the type used here can detect neuronal spikes from a distance of 50-60 μm at best [44]. The field strength produced by myocytes is much larger, correspondingly a greater horizon of the electrode must be assumed. However, the contribution of distant cells to the local FP decreases according to the cable equation as a function of the intercellular resistance. We demonstrated that cells locally, in the surrounding of one electrode, exhibited similar waveforms and that AP characteristics correlated, likewise locally, with the FP. Therefore the results support the interpretation, that, within the limits of the technique, the populations of cells are locally homogenous.

Yet we do see a change of the FP waveform as the activity propagates through the culture with increased values of FP_{rise} at the origin of excitation on the MEA. The FP found at this electrode, representing a local average of the single cell properties indicates that the majority of the cells display slow AP rise times and are therefore most probably pacemaker-like APs. Thus, although we assume and demonstrated local homogeneity of the cells, this does not preclude us to detect changes of the composition of local populations in different regions of the culture.

Conclusion

We could demonstrate with our experiments that intrinsic AP parameters like AP duration and AP rise time can be characterized inside a multicellular preparation of cardiac myocytes from localized extracellular recordings of FPs. The contribution of individual transmembrane currents to the AP and their change could be distinguished in the FP waveform and the FP parameters could be used to characterize regional electrophysiological differences in the culture. Although the interpretation of the FP components does not reveal absolute values for AP properties or currents, it can assist in the analysis of the contribution of the different electrophysiological parameters and their modulation in association with physiological and pathophysiological changes of excitation generation and excitation spread in multicellular preparations of cardiac myocytes.

Abbreviations

AP (action potential), APD90 (duration of the intracellular recorded action potential at 90% repolarization), AP_{rise} (action potential rise time), ISI (Inter-spike interval), FP (field potential), FP_{dur} (duration of the FP from the peak time of FP_{MIN} to the peak time of FP_{MAX}), FP_{MAX} (last positivity in an FP cycle), FP_{MIN} (first negativity of the FP), FP_{slow} (second negativity of the FP), FP_{pre} (positive peak preceding FP_{MIN}), FP_{rise} (falling phase of the FP), MEA (microelectrode array), V_{max} (maximum upstroke velocity of the AP).

Acknowledgements

This research was supported by the BMBF (FKZ 0310967, 0310965, and 0310964D). Dr. K. Banach was funded by the Lise Meitner-Habilitationsstipendium of Nordrhein Westfalen.

References

1 Cohen ML, Hoyt RH, Saffitz JE, Corr PB: A high density in vitro extracellular electrode array: description and implementation. Am J Physiol 1989:257:H681-H689.

2 Schmitt C, Ndrepepa G, Deisenhofer I, Schneider M: Recent advances in cardiac mapping techniques. Curr Cardiol Rep 1999;1:149-156.

3 Schuessler RB, Kawamoto T, Hand DE, Mitsuno M, Bromberg BI, Cox JL, Boineau JP: Simultaneous epicardial and endocardial activation sequence mapping in the isolated canine right atrium. Circulation 1993;88:250-263.

4 Sahakian AV, Peterson MS, Shkurovich S, Hamer M, Votapka T, Ji T, Swiryn S: A simultaneous multichannel monophasic action potential electrode array for in vivo epicardial repolarization mapping. IEEE Trans Biomed Eng 2001;48:345-353.

5 Schalij MJ, van Rugge FP, Siezenga M: Endocardial activation mapping of ventricular tachycardia in patients: first application of a 32-site bipolar mapping electrode catheter. Circulation 1998;98:2168-2179.

6 Shibata N, Inada S, Mitsui K, Honjo H, Yamamoto M, Niwa R, Boyett MR, Kodama I: Pacemaker shift in the rabbit sinoatrial node in response to vagal nerve stimulation. Exp Physiol 2001;86:177-184.

7 Boyett MR, Honjo H, Kodama I: The sinoatrial node, a heterogeneous pacemaker structure. Cardiovasc Res 2000;47:658-687.

8 Rohr S, Kucera JP, Kleber AG: Slow conduction in cardiac tissue, I: effects of a reduction of excitability versus a reduction of electrical coupling on microconduction. Circ Res 1998;83:781-794.

9 Hubbard JI, Llinas R, Quanstel DMJ: Electrophysiological analysis of synaptic transmission. London, Edward Arnold, 1969.

10 Regehr WG, Pine J, Cohan CS, Mischke MD, Tank DW: Sealing cultured invertebrate neurons to embedded dish electrodes facilitates long-term stimulation and recording. J Neurosci Meth 1989;30:91-106.

11 Omura Y: Relationship between transmembrane action potentials of single cardiac cells and their corresponding surface electrograms in vivo and in vitro, and related electromechanical phenomena. Trans N Y Acad Sci 1970;32:874-910.

12 Henze DA, Borhegyi Z, Csicsvari J, Mamiya A, Harris KD, Buzsaki G: Intracellular features predicted by extracellular recordings in the hippocampus in vivo. J Neurophysiol 2000;84:390-400.

13 Banach K, Halbach MD, Hescheler J and Egert U: In-vitro development of a mouse heart: Functional differentiation of electrical activity in cardiac myocytes derived from embryonic mouse heart. Am J Physiol 2003;284:H2114-H2123.

14 Igelmund P, Fleischmann BK, Fischer IR, Soest J, Gryshchenko O, Bohm-Pinger MM, Sauer H, Liu Q, Hescheler J: Action potential propagation failures in long-term recordings from embryonic stem cell-derived cardiomyocytes in tissue culture. Pflügers Arch 1999;437:669-679.

15 Isenberg G, Klockner U: Calcium tolerant ventricular myocytes prepared by pre-incubation in a "KB medium". Pflügers Arch 1982;395:6-18.
16 Maltsev VA, Wobus AM, Rohwedel J, Bader M, Hescheler J: Cardiomyocytes differentiated in-vitro from embryonic stem cells developmentally express cardiac- specific genes and ionic currents. Circ Res 1994;75:233-244.
17 Hamill OP, Marty A, Neher E, Sakmann B, Sigworth FJ: Improved patch-clamp techniques for high-resolution current recording from cells and cell-free membrane patches. Pflügers Arch 1981;391:85-100.
18 Egert U, Schlosshauer B, Fennrich S, Nisch W, Fejtl M, Knott T, Mueller T, Hämmerle H: A novel organotypic long-term culture of the rat hippocampus on substrate-integrated multielectrode arrays. Brain Res Prot 1998;2:229-242.
19 Egert U, Knott T, Schwarz C, Nawrot M, Brandt A, Rotter S, Diesmann M: MEA-Tools: an open source toolbox for the analysis of multi-electrode data with MATLAB. J Neurosci, Meth 2002;117:33-42.
20 Feld Y, Melamed-Frank M, Kehat I, Tal D, Marom S, Gepstein L: Electrophysiological modulation of cardiomyocytic tissue by transfected fibroblasts expressing potassium channels: A novel strategy to manipulate excitability. Circulation 2002;105:522-529.
21 Hescheler J, Wartenberg M, Fleischmann BK, Banach K, Acker H, Sauer H: Embryonic stem cells as a model for the physiological analysis of the cardiovascular system. Methods Mol Biol 2002;185:169-87.
22 Dumitru D: Physiologic basis of potentials recorded in electromyography. Muscle Nerve 2000;23:1667-1685.
23 Spach MS, Barr RC, Serwer GA, Kootsey M, Johnson EA: Extracellular potentials related to intracellular action potentials in the dog prukinje system. Circ Res 1972;30:505-519.
24 Yamamoto M, Honjo H, Niwa R, Kodama I: Low-frequency extracellular potentials recorded from the sinoatrial node. Cardiovasc Res 1998;39:360-372.
25 Cai D, Winslow RL, Noble D: Effects of gap junction conductance on dynamics of sinoatrial node cells: two-cell and large-scale network models. IEEE Trans Biomed Eng 1994;41:217-231.
26 Verheijck EE, Wilders R, Joyner RW, Golod DA, Kumar R, Jongsma HJ, Bouman LN, van Ginneken ACG: Pacemaker synchronization of electrically coupled rabbit sinoatrial node cells. J Gen Phys 1998;111:95-112.
27 Taccardi B, Veronese S, Franzone PC, Guerri L: Multiple components in the unipolar electrogram: a simulation study in a three-dimensional model of ventricular myocardium. J Cardiovasc Electrophysiol 1998;9:1062-1084.
28 Bers DM: Excitation-contraction coupling and cardiac contractile force. Kluwer Academic Publishers, Netherlands, 2nd edition; 2001.
29 Hiraoka M, Sawanobori T, Kawano S, Hirano Y, Furukawa T: Functions of cardiac ion channels under normal and pathological conditions. Jpn Heart J 1996;37:693-707.
30 Lipsius SL, Hueser J, Blatter AL: Intracellular Ca^{2+} release sparks atrial pacemaker activity. News Physiol Sci 2001;16:101-106.
31 Spach MS, Miller WT 3rd, Miller-Jones E, Warren RB, Barr RC: Extracellular potentials related to intracellular action potentials during impulse conduction in anisotropic canine cardiac muscle. Circ Res 1979;45:188-204.
32 Schouten VJ, ter Keurs HE: The slow repolarization phase of the action potential in rat heart. J Physiol 1985;360:13-25.
33 Cribbs LL, Martin BL, Schroder EA, Keller BB, Delisle BP, Satin J: Identification of the t-type calcium channel (Ca(v)3.1d) in developing mouse heart. Circ Res 2001;88:403-407.
34 Haberl R, Steinbeck G, Luderitz B: Comparison between intracellular and extracellular direct current recordings of sinus node activity for evaluation of sinoatrial conduction time. Circulation 1984;70:760-767.
35 Wang L, and Duff HJ: Developmental changes in transient outward current in mouse ventricle. Circ Res 1997;81:120-127.
36 Chandler WK, Meves H: Voltage clamp experiments on internally perfused giant axons. J Physiol 1965;180:788-820.
37 Leitch SP and Brown HF: Effect of raised extracellular calcium on characteristics of the guinea-pig ventricular action potential. J Mol Cell Cardiol 1996;26:541-551.
38 Boyett MR, Honjo H, Yamamoto M, Nikmaram MR, Niwa R, Kodama I: Downward gradient in action potential duration along conduction path in and around the sinoatrial node. Am J Physiol 1999;276:H686-H698.
39 Cramer M, Hariman RJ, Boxer R, Hoffman BF: Electrograms from the canine sinoatrial pacemaker recorded in vitro and in situ. Am J Cardiol 1978;42:939-946.
40 Honjo H, Lei M, Boyett MR, Kodama I: Heterogeneity of 4-aminopyridine-sensitive current in rabbit sinoatrial node cells. Am J Physiol 1999;276:H1295-H1304.
41 Temte JV, Davis LD: Effect of calcium concentration on the transmembrane potentials of purkinje fibers. Circ Res 1967;20:32-44.
42 Satin J, Fujii S, DeHaan R: Development of cardiac beat rate in early chick embryos is regulated by regional cues. Dev Biol 1988;129:103-113.
43 Those N, Yokoshiki H, Sperelakis N: Developmental changes in ion channels. In Sperelakis N (ed) Cell Physiology Source Book, 2nd ed. San Diego, Ca: Academic Press, 1998, pp 518-531.
44 Egert U, Heck D, Aersten A: 2-Dimensional monitoring of spiking networks in acute brain slices. Exp Brain Res 2002;142:268-274.